https://doi.org/10.5194/bg-2023-169
Preprint. Discussion started: 21 September 2023

Biogeosciences Discussions
Open Access
EGU

POTENTIAL IMPACTS OF CABLE BACTERIA ACTIVITY ON HARD-SHELLED BENTHIC FORAMINIFERA: A PRELUDE TO IMPLICATIONS FOR THEIR INTERPRETATION AS BIOINDICATORS OR PALEOPROXIES

Maxime Daviray[1]*, Emmanuelle Geslin[1], Nils Risgaard-Petersen[2], Vincent V. Scholz[3], Marie Fouet[1,4], Edouard Metzger[1]

*Correspondence: Maxime DAVIRAY (maxime.daviray@univ-angers.fr)

1. UMR CNRS 6112 - LPG, **Université d'Angers**, Nantes Université, Le Mans Université, CNRS, 49000 Angers, France
2. Aquatic Biology, Department of Biology, Aarhus University, 8000 Aarhus C, Denmark
3. Center for Electromicrobiology, Department of Biology, Aarhus University, 8000 Aarhus C, Denmark
4. at present: UMR CNRS 5805 EPOC - OASU, Station Marine d'Arcachon, Université de Bordeaux, CNRS, 33120 Arcachon, France

ABSTRACT

Cable bacteria (CB) are filamentous bacteria coupling sulphide oxidation to oxygen reduction over centimetre distances. This bacterial activity generates a strong pH gradient within the first few centimetres of the sediment that affects the microhabitats occupied by benthic foraminifera. Hard-shelled foraminifera are protists able to build a calcareous or agglutinated shell (called "test"). Here we study the impact of sediment acidification induced by CB activity (CBA) on calcareous test preservation. For this study, sediment cores were sampled in the macrotidal Auray estuary located on the French Atlantic coast. Living and dead foraminifera were quantified (until 5-cm depth) and discriminated using the Cell-Tracker™ Green vital marker. CBA was assessed with pH and oxygen profiles combined with quantitative Polymerase Chain Reaction (q-PCR). On two different intertidal mudflats, volumetric filament densities have been measured. They were comparable to those observed in the literature for coastal environments, with 7.4 ± 0.4 and 74.4 ± 5.0 $m.cm^{-3}$ per bulk sediment respectively. Highly contrasting CBA (from low to very intense) were described with lowest pH at 5.8. This seems to lead to various dissolution stages of the foraminiferal calcareous test from intact to fully dissolved tests revealing the organic lining. The dissolution scale is based on observations of living *Ammonia* spp. and *Haynesina germanica* specimens under a Scanning Electronic Microscope. Furthermore, dead foraminiferal assemblages showed a strong calcareous test loss and an organic lining accumulation throughout depth under low pH, hampering the test preservation in deep sediment. These changes in both living and dead foraminiferal assemblages imply that CB must be strongly considered in ecological monitoring and historical studies using foraminifera as bioindicator and paleoenvironmental proxy.

https://doi.org/10.5194/bg-2023-169
Preprint. Discussion started: 21 September 2023


Biogeosciences
Discussions
Open Access
EGU

1 INTRODUCTION

Cable bacteria (CB) were discovered by Pfeffer and co-workers in 2012. They are sulphide-oxidizing filamentous multicellular procaryotes from the Desulfobulbaceae family. They live in marine and freshwater sediments all around the world (Risgaard-Petersen et al., 2015; Burdorf et al., 2017). They inhabit a several centimetres thick zone from the oxic surface to the deep sulphidic sediment. CB generate a vertical bioelectrical current by coupling the cathodic oxygen or nitrate reduction at the sediment surface to the anodic sulphide oxidation at depth (Nielsen et al., 2010; Pfeffer et al., 2012; Risgaard-Petersen et al., 2012; Marzocchi et al., 2014). CB activity (CBA) strongly affects sediment geochemistry and results in a clear geochemical fingerprint: an oxygen decrease in the surface sediments combined with a pH maximum in this oxic zone, followed by a strong acidification of the pore water in the suboxic zone (Nielsen et al., 2010; Risgaard-Petersen et al., 2012, 2014; Meysman et al., 2015). It leads to iron sulphide and carbonate dissolution from the suboxic zone (Risgaard-Petersen et al., 2012; Rao et al., 2016; van de Velde et al., 2016) and possibly the calcareous shell of benthic organisms.

Benthic foraminifera are unicellular meiofaunal organisms. Most species can build a hard-shell (called a test) that can be agglutinated (cemented grains), hyaline calcareous (calcium carbonate) and porcelaneous calcareous (calcium carbonate enriched in magnesium). Benthic foraminifera are very abundant in marine areas (Martin, 2000) including transitional environments (Alve & Murray, 1999; Debenay et al., 2006). These systems located between marine and continental areas (i.e. littoral and estuarine zones), are subjected to a high variability of environmental factors (e. g. tide, freshwater flows, evaporation, development of seagrass meadows over seasonal cycles...). Then, benthic foraminifera are submitted to strong variability of physical and geochemical parameters such as temperature, salinity or pH that they must tolerate. Despite such variability, benthic foraminifera assemblages have been used in transitional environments as bioindicators for biomonitoring ecological state (Mojtahid et al., 2006; Balsamo et al., 2012; O'Brien et al., 2021; Fouet et al., 2022) and as paleoenvironmental proxies to understand past ecosystems functioning (Martin, 2000; Murray, 2006; Katz et al., 2010; Keul et al., 2017; Durand et al., 2018). However, species with a calcareous test can be affected by low pH and carbonate undersaturation leading to test dissolution (Le Cadre et al., 2003; Bentov et al., 2009; de Nooijer et al., 2009; Haynert et al., 2011, 2014; Kurtarkar et al., 2011; Charrieau et al., 2018b). Even if they are rarely observed *in situ*, few studies have reported signs of severe test dissolution in living assemblages (e.g., Alve and Nagy, 1986; Buzas-Stephens, 2005; Polovodova and Schonfeld, 2008; Haynert et al., 2012; Cesbron et al., 2016; Charrieau et al., 2018a; Schönfeld and Mendes, 2022). These authors attribute these dissolution observations to low pH and undersaturation of the carbonate

https://doi.org/10.5194/bg-2023-169
Preprint. Discussion started: 21 September 2023


Biogeosciences
Discussions
Open Access
EGU

system, which would be due to abiotic conditions (anthropogenic pollution, freshwater intrusions) or more rarely to biotic ones (degradation of plants). Under laboratory conditions, Le Cadre et al (2003) have shown that test dissolution of living *Ammonia becarri* starts at pH 7.5.

Benthic foraminifera live mainly in the topmost sediment. CB develop also on the few topmost centimetres of the sediment, which can therefore lead to an environmental overlap of the bacterial and foraminiferal communities. Richirt et al 2022 hypothesised that CBA induces the dissolution of calcareous tests within the sediment of the Lake Grevelingen (Netherlands). In the present study, we assess the impact of cable bacteria activity on the foraminiferal test preservation in sediment, testing the hypothesis that CBA is responsible for depleting the preservation of calcareous foraminifera in benthic assemblages. To achieve this, CBA was characterized by oxygen and pH microprofiling and CB density quantified by qPCR on intertidal mudflats of the Auray estuary (French Atlantic coast). Calcareous test dissolution stages were defined and quantified thanks to the analyse of SEM images. Then, we described living and dead foraminiferal assemblages to assess the calcareous test loss.

https://doi.org/10.5194/bg-2023-169
Preprint. Discussion started: 21 September 2023

2 MATERIALS AND METHODS

2.1 Studied Area

The Gulf of Morbihan (Atlantic coast, France) is an enclosed marine bay where the Auray river flows. The Auray estuary is a macrotidal estuary with a tide range about 4 m (**Figure 1**).

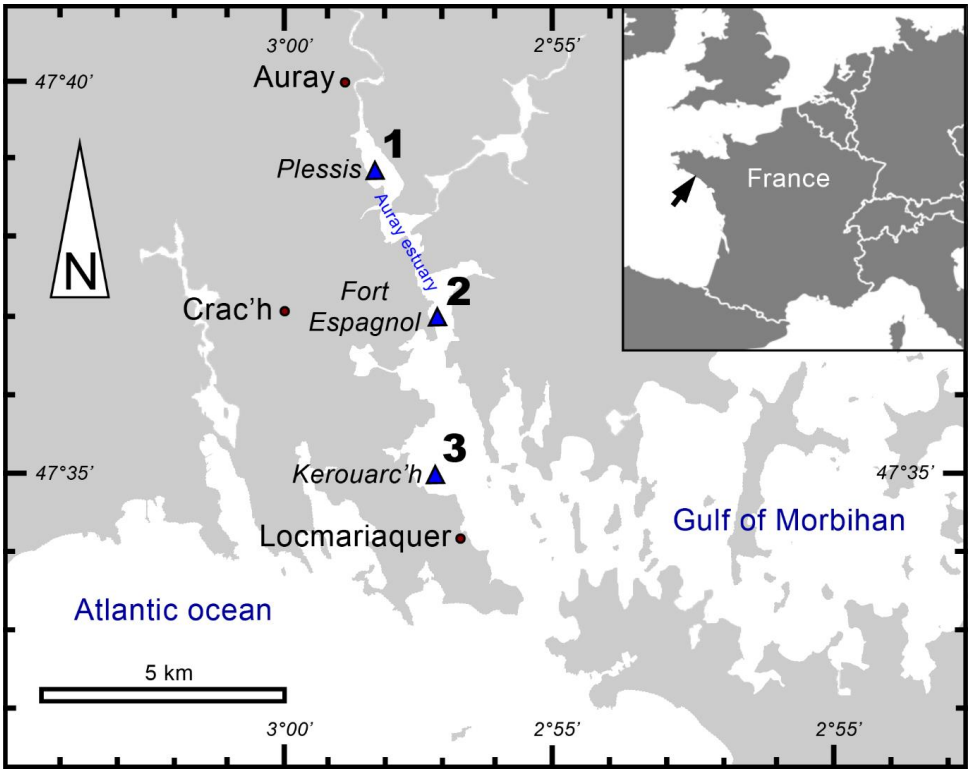

Figure 1. Locations of sampling stations in the intertidal mudflats of the Auray estuary (France).

Saltwater flows upstream over 20 km from the mouth of the estuary (357 m wide) which is tide-dominated (online data from OFB and IFREMER, accessed on May 05th 2022). The extensive description of this area was made by Fouet et al. (2022).

In September 2020, three stations along the Auray estuary were sampled on intertidal mudflats at low tide (**Figure 1** and **Table 1**): station 1 (Plessis), station 2 (Fort Espagnol) and stations 3 (Kerouarc'h). Characteristics of the sampled stations are presented in **Table 1**.

Table 1. Characteristics of the stations sampled in September 2020. *Temperature and salinity values correspond to these measured on the sampling day; weighted average and SD of sediment density data from a previous campaign in 2019; (*) name of the station after Fouet et al., (2022).*

Station	Coordinates	Distance from Sea	T (°C)	Salinity	Sediment Density ($g.cm^{-3}$)	Vegetation Cover
1	47.646° N,	12 km	24.4	29.6	1.71 ± 0.12	*Ulvea* mat

https://doi.org/10.5194/bg-2023-169
Preprint. Discussion started: 21 September 2023

(*6B)	-2.972° W					
2 (*4B)	47.616° N, -2.953° W	8 km	21.2	38.5	1.67 ± 0.33	*Ulvea* mat
3 (*2C)	47.583° N, -2.955° W	4.3 km	21.5	34.3	1.51 ± 0.23	thick *Ulvea* mat few *Zostera*

2.2 Sediment Sampling and Processing

One core was sampled from each station by hand with a Plexiglas® tube (82 mm inner diameter, 50 mm depth) and was transported within an hour in a cool box to the field laboratory. Then, the cores were submerged in ambient seawater for at least two hours to retrieve *in situ* conditions before microprofiling.

After microprofiling, each core was sliced using a core pusher and two trowels. Slice thickness was 2 mm for the first 20 mm depth, and 10 mm up to 50 mm depth. Each sediment slice was treated with Cell-Tracker™ Green (CTG 5 CMFDA: 5-chloromethylfluorescein diacetate; Molecular Probes, Invitrogen Detection Technologies) to mark living benthic foraminifera by fluorescence (Bernhard and Bowser, 1996; Bernhard et al., 2006). One mg of CTG was dissolved in 1 mL of dimethylsulfoxide (DMSO). This solution was then pipetted into the flask containing the sediment slice and its volume of ambient water to get a final solution of CTG about 1 µM (Bernhard et al., 2006; Pucci et al., 2009; Langlet et al., 2013, 2014; Cesbron et al., 2016). Each sample was then incubated in dark at room temperature overnight and then fixed with ethanol 99% (Choquel et al., 2021). Eventually, the samples were sieved with tap water over 315-, 150-, 125- and 63-µm mesh screens. Samples were conserved in 99% ethanol.

DNA was extracted from sub-samples of sediment slices at stations 1 and 2. 1-2 g every second slice down to 18-mm depth were sampled with a heat-sterilized spatula and transferred to 2 ml Eppendorf tubes, then frozen at -20°C degrees. Samples were sent in dry ice ($CO_{2(s)}$ at -50°C) to the Microbiology Institute of Biology in Aarhus University (Denmark) for qPCR analysis to quantify cable bacteria biomass.

2.3 Microsensor Profiling

Two Unisense© profiling systems were used simultaneously. One consisted of two oxygen Clark-type microsensors with a 50 µm tip (Revsbech and Jørgensen, 1986; Revsbech, 1989), and the other of a pH sensor with a 500 µm tip diameter (PH500, Unisense). They were both mounted on a motorized micromanipulator linked to a computer, and connected to a MultiMeter S/N. The increment was 50 µm until 3 mm for oxygen. It was 100 µm around the seawater-sediment interface (SWI) for pH, and it was adapted in real time according to the evolution of the observed profile until 50 mm depth. For each core, eight descents were managed for O_2,

https://doi.org/10.5194/bg-2023-169
Preprint. Discussion started: 21 September 2023

for a total of 16 profiles, while only one profiling was done for pH. To calibrate the O_2 microsensor, two points were measured, with the 100% of oxygen saturation in the bubbling seawater column, and the 0% into the anoxic part of sediment. To calibrate the pH microsensor, 3 NBS buffers were used (values 4.0, 7.0, 9.2).

2.4 Living Foraminiferal Analyses

Counts of hard-shell benthic foraminifera were performed in wet conditions (water) on the >125 µm fractions using an epifluorescence stereomicroscope (Olympus SZX12 with a light source CoolLED *p*E-100, emission wavelength λ = 470 nm). All specimens showing clear green fluorescence were picked and identified. Remaining specimens were considered as dead. In doubtful cases, particularly with agglutinated species, specimens were crushed to inspect whether fluorescence was due to the presence of protoplasm, to the autofluorescence of sediment grains composing the test, or the presence of bacteria or nematodes living inside (Langlet et al., 2013; Cesbron et al., 2016). Total foraminiferal densities were expressed per 50 cm^2 of sediment and foraminiferal densities for sediment layers per 10 cm^3 volume.

For the taxonomy of hard-shell foraminifera species, reference publications on estuarine foraminifera (Feyling-Hanssen et al, 1972; Hansen et al, 1976; Murray et al, 1979; Scott et al, 1980; Hayward et al, 2004; Schweizer et al, 2011; Camacho et al, 2015; Richirt et al, 2019; Fouet et al., 2022; Jorissen et al., 2023), and the World Register of Marine Species were used. The distinction between the *Ammonia* phylotypes (Richirt et al, 2019) being difficult, on particular on the dissolved tests, the results will be discussed at the genus level.

2.5 SEM Imaging

Living foraminifera from three layers (0-2 / 6-8 / 40-50 mm depth), according to main pH features, were all observed under a Scanning Electronic Microscope (SEM). Two different high-resolution SEM were used: a DEBEN Hitachi TM4000 at the LPG (samples not metallised, 15kV, wd = 6,5 mm, partial vacuum (60 Pa)) and a Zeiss EVO LS10 at the Service Commun d'Imageries et d'Analyses Microscopiques of Angers University (SCIAM; samples not metallised, 20 kV, wd = 6,5 mm, partial vacuum (60 Pa), amperage 200 to 250 pA). Few scales of calcareous test dissolution of living foraminifera have been proposed in the literature (Corliss and Honjo, 1981; Le Cadre, 2003b; Haynert et al., 2011; Gonzales et al., 2017; Charrieau et al., 2018c; Schönfeld and Mendes, 2022). These authors proposed scales varying from 4 to 5 different stages based on SEM images or stereomicroscope observations. They used a wide variety of morphological criteria to describe each dissolution stage (i.e. the number of calcite layers altered and chambers damaged, the presence of cracks or holes, whether the inner organic lining was visible, etc.). In the present study, we propose a scale of six dissolution

https://doi.org/10.5194/bg-2023-169
Preprint. Discussion started: 21 September 2023

stages based on SEM pictures of the two most abundant calcareous species in our living assemblages (*Ammonia* spp. and *Haynesina germanica*).

Table 2. Description of the six dissolution stages of the calcareous tests of Ammonia spp. and Haynesina germanica.

Dissolution Stage	Name	SEM Observations and Stage Descriptions	Figures
DS-0	Intact test	intact, glassy test with a smooth surface and cylindrical pores, no sign of dissolution.	**Fig. 3-1** **Fig. 4-1**
DS-1	Slight surface dissolved test	transparent test with cylindrical pores, alteration of the last calcite layer only, appearance of the interpore sutures in *H. germanica* (scarce in *Ammonia* spp., alteration more visible on the inter-chamber walls).	**Fig. 3-2** **Fig. 4-2**
DS-2	Peeled test	dull, whitish test with some fusion of adjacent widen pores, calcite layers cracking and crumbling, last chamber often lost, thinner and blunt tubercular ornamentation of *H. germanica.*	**Fig. 3-3** **Fig. 4-3**
DS-3	Cracked test	opaque and cracked test with a strong alteration of all calcite layers, brittle test with holes, fusion of widen pores, the organic lining can be visible, loos of last chamber, broken ornamentation of *H. germanica.*	**Fig. 3-4** **Fig. 4-4**
DS-4	"Star-shape" test	nearly completely dissolved test, only the inter-chamber walls remaining, the last chambers often absent, dissolved peripheral chambers with the inner organic lining visible.	**Fig. 3-5** **Fig. 4-5**
DS-5	Fully dissolved test	totally dissolved test revealing the inner organic lining, may keep the foraminifera shape allowing the identification of the genus *Ammonia* (not observed for *H. germanica*).	**Fig. 3-6**

https://doi.org/10.5194/bg-2023-169
Preprint. Discussion started: 21 September 2023

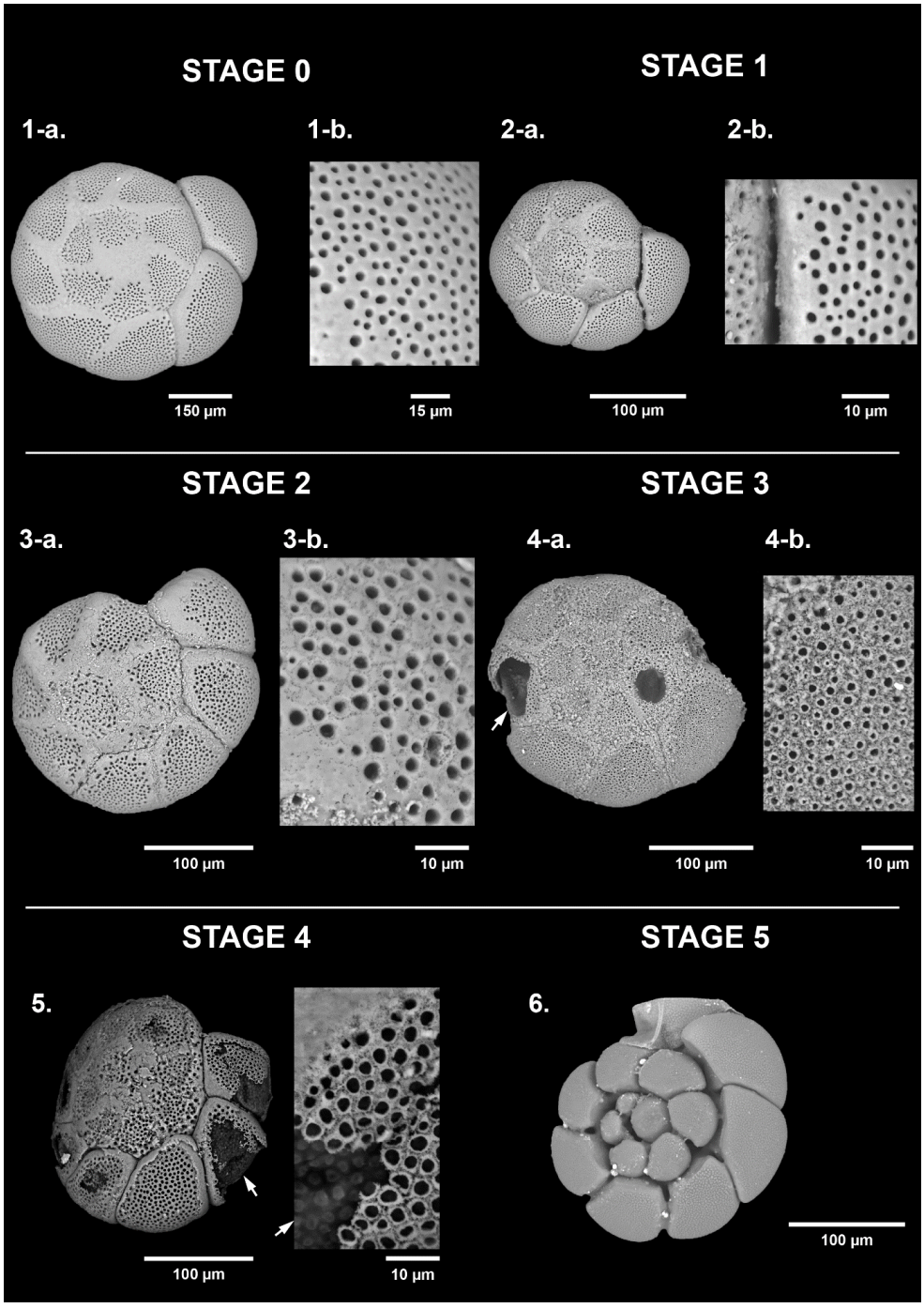

Figure 2. Dissolution scale of Ammonia spp. based on high-resolution SEM images (spiral view). *The specimens are classified into six stages of test dissolution from intact (stage 0) to fully dissolved (stage 5). For stages 0 to 2, a zoom on the last formed chamber was done* ***(1-b, 2-b, 3-b)****, and on the n-1 chamber for stage 3* ***(4-b)****. White arrows point the organic lining.*

https://doi.org/10.5194/bg-2023-169
Preprint. Discussion started: 21 September 2023

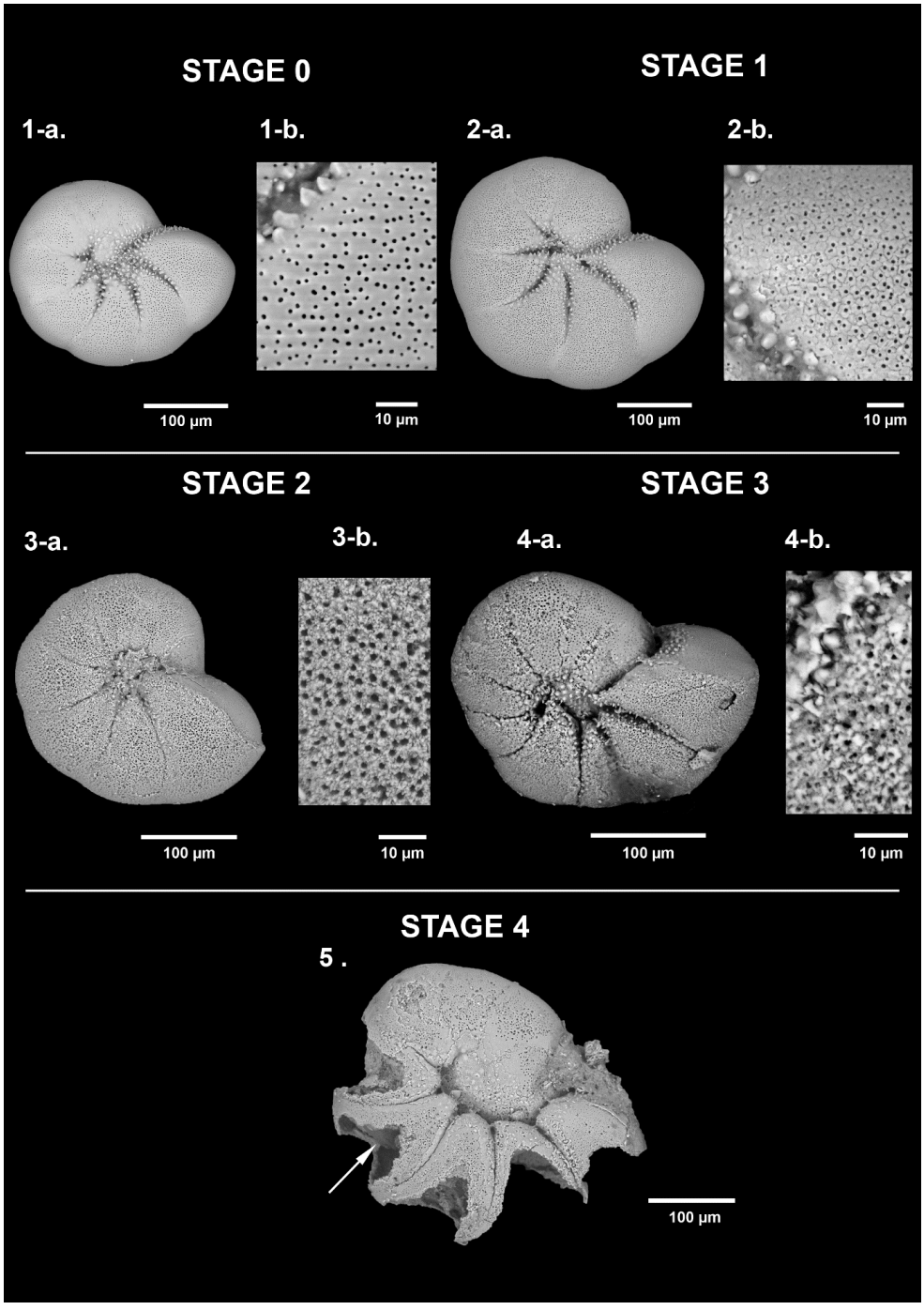

Figure 3. Dissolution scale of Haynesina germanica based on high-resolution SEM images. *The specimens are classified into five stages of test dissolution from intact (stage 0) to the « star shape » (stage 4). No organic lining (stage 5) has been identified as belonging to the taxa Haynesina. For stages 0 and 1, a zoom on the last formed chamber was done (**1-b, 2-b**), and on the n-1 chamber for stages 2 and 3 (**3-b, 4-b**). White arrow points the organic lining.*

https://doi.org/10.5194/bg-2023-169
Preprint. Discussion started: 21 September 2023

2.6 Dead Foraminiferal Analyses

Non fluorescent tests of foraminifera were counted as dead specimens and picked in wet conditions (water) to preserve the organic linings from fully dissolved tests. We proceeded under a stereomicroscope (ZEISS Stemi sv11) in three sediment layers: the surface layer (0-2 mm), the subsurface layer (6-8 mm) and the deep layer (40-50 mm). After quick observations, when high densities were estimated (above 500 individuals; Patterson and Fishbein, (1989)) fractions were splitted into 8 sub-samples using a wet splitter (Charrieau et al., 2018a).

2.7 Ratios in Foraminiferal Assemblages

In order to characterize the loss of calcareous in the assemblages, we defined a ratio as follows:

$$C/T = \textit{calcareous foraminifera/total foraminifera}$$

Calcareous foraminifera are counted regardless their dissolution stage and total foraminifera include agglutinated individuals. To estimate the intensity of dissolution in the assemblage, we calculated the following ratio:

$$DS\text{-}5/C = \textit{calcareous test at dissolution stage 5/total calcareous foraminifera}$$

These ratios were calculated on both living and dead assemblages for layers 0-2 / 6-8 and 40-50 mm.

2.8 Statistical Procedure

The putative relationship between CBA and the advanced dissolution stages of the living calcareous test foraminifera was assessed by applying the parametric Fisher's test followed by the pair-wise Fisher's test for *post-hoc* comparisons were used. To minimize the risk type 1 error *p*-values were FDR-adjusted. The significance level was set to 5 %. As the last layer of calcite produced during the growth of the foraminifera covers the entire test and is thinner than the others (Haynes, 1981; Hansen, 1999; Debenay et al., 2000; Boudagher-Fadel, 2018), DS-1 and 2 are more commonly observed resulting from a process of gradual dissolution or precipitation of calcite. Discrimination of the effect of the dissolution process is therefore made on the alteration of several calcite layers as for DS-3 and above. For this purpose, the dissolution stages were combined into two groups: no to slight dissolution (DS-0, 1 and 2) and moderate to severe dissolution (DS-3, 4 and 5). These two groups were then compared between each of the three stations, and between the different depth levels (0-2 / 6-8 / 40-50 mm depth) for each station. Statistics were carried out using the *R* software using the "stats" and "rstatix" packages.

https://doi.org/10.5194/bg-2023-169
Preprint. Discussion started: 21 September 2023

2.9 Sediment Treatment for DNA Extraction and Quantification

DNA was extracted from weighed amounts of sediment (0.22 - 0.25 g wet weight). DNA extraction was carried out using DNeasy PowerLyzer PowerSoil Kit (Qiagen) and the DNA was collected in 60 µl elution buffer. The analysis followed the procedures outlined in Geelhoed et al. (2020). The primer combination of ELF645wF and CB836wR was used to target the 16S rRNA gene of the marine cable bacteria of the genus *Candidatus* Electrothrix Trojan, 2016. The calibration curves were obtained using a synthetic standard (sequence accession KR912339.1, position 611-912, synthesized by Eurofins Genomics, Denmark) diluted in a 10-fold dilution series. The standards and samples were run in triplicates. Each reaction contained the master mix (RealQ Plus 2x Master Mix Green, Low ROXTM, Ampliqon, Denmark), forward and reverse primers (0.2 µM), BSA (1 µM). The qPCR was performed with a real time PCR analyser (AriaMX, Agilent). The thermal cycles were as follows: 15 min at 95 °C for initial denaturation followed by 40 cycles of 15 s at 95 °C (denaturation), 30 s at 60 °C (annealing), and 20 s at 72 °C (amplification). Afterwards, the melting curve was obtained by 30 s at 95°C, 30 s at 60 °C, and 30 s at 95 °C. Finally, the temperature was held for 5 min at 40 °C to terminate the analysis. The results are reported as the unit gene copies.(g wet sediment) $^{-1}$. CB filament density were calculated as in Geelhoed et al. (2020), using data of wet sediment density from a previous campaign in 2019 (**Table 1**), and expressed in m.cm^{-3}.

3 RESULTS

3.1 Microsensor Profiles and Cable Bacteria Abundance

Oxygen penetration depth in the sediment at stations 1, 2 and 3 was 1.4 ± 0.2, 0.9 ± 0.3 and 0.9 ± 0.2 mm, respectively. At station 1, pH rapidly decreased from 7.7 at the Sea Water Interface (SWI) to a minimum of 6.8 at 15 mm depth. Below this minimum, pH stabilised to 7.2 around 40 mm depth. In contrast, at stations 2 and 3, pH increased immediately below the SWI from 7.8 to 8.1 at 0.8 mm depth and to 7.95 at 0.6 mm, respectively (**Figure 4**). Below these maxima, at both stations, pH reached a minimum of 5.8 at 7 mm depth at station 2 and of 6.3 between 7-19 mm depth at station 3. Below these minima, pH stabilised at 6.8 after 25 mm depth at station 2, and at 6.9 after 34 mm depth at station 3. Those profiles with an oxygen decrease in the surface sediments combined with a pH maximum in this oxic zone, followed by a strong acidification of the pore water in the suboxic zone, are typical CBA fingerprints.

At station 1, the number of 16S CB copies of *Candidatus* Electrothrix ranged from 0.23 ± 0.01 $_x10^7$ to 0.48 ± 0.01 $_x10^7$ 16S copies.(g wet sediment)$^{-1}$, and remained constant through depth (**Figure 4**). At station 2, it amounted to 2.8 ± 0.12 $_x10^7$ 16S copies.(g wet sediment)$^{-1}$ in the upper 5 mm of sediment and progressively decreased to about 0.3 ± 0.01 $_x10^7$ 16S

https://doi.org/10.5194/bg-2023-169
Preprint. Discussion started: 21 September 2023

copies.(g wet sediment)$^{-1}$ in the 16-18 mm depth layer. The maximum 16S CB copies of *Ca.* Electrothrix in station 2 corresponded to the maximum pH in depth. According to Gelhoed et al. (2020) and using sediment density from the same stations obtained in 2019 (pers. comm. M. Fouet), we calculated a CB density of 7.4 ± 0.4 and 74.4 ± 5.0 m.cm^{-3} at stations 1 and 2 respectively.

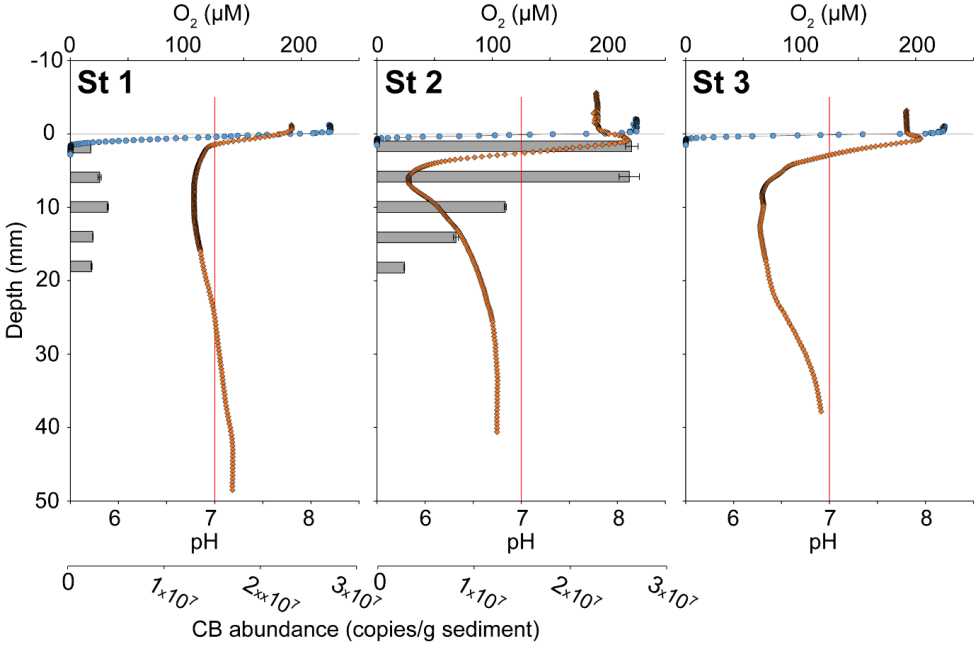

Figure 4. Sediment oxygen (blue circles) and pH (orange diamonds) microprofiles at the three stations, and vertical distribution of cable bacteria abundance (qPCR of Ca. Electrothrix 16S rRNA gene copies, grey bars) for stations 1 and 2. *0 is the position of the Sea Water Interface (SWI). The vertical red line represents neutral pH. The oxygen profile presented is one of those obtained by microprofiling, and representative of O_2 penetration for each station.*

3.2 Hard-Shelled Benthic Foraminiferal

3.2.1 Living Foraminiferal Diversities and Densities

The foraminiferal species assemblages were typical of the estuarine environments (Debenay et al., 2000), with a poor species richness (14, 13 and 18 species at stations 1, 2 and 3 respectively). *Ammonia* spp. and *Haynesina germanica* (Ehrenberg, 1840) both strongly dominated the assemblages at all three stations (25.1 and 51.5 % respectively of the total assemblage for station 1, 14.5 and 48.2 % for station 2, 7.3 and 61.4% for station 3; **Figure 5**). *Ammonia* spp. included the species *Ammonia veneta* (Schultze, 1854) (phylotype T1 after Hayward et al., 2004), *Ammonia aberdoveyensis* Haynes, 1973 (phylotype T2 after Hayward et al., 2004), and *Ammonia confertitesta* Zheng, 1978 (phylotype T6 after Hayward et al., 2004). Agglutinated foraminifera represent 19.9, 25.7 and 12.7 % of the total assemblage at

https://doi.org/10.5194/bg-2023-169
Preprint. Discussion started: 21 September 2023

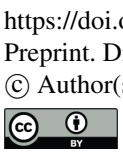

250 stations 1, 2 and 3, respectively. They were dominated by *Ammobaculites agglutinans*
251 (d'Orbigny, 1846).

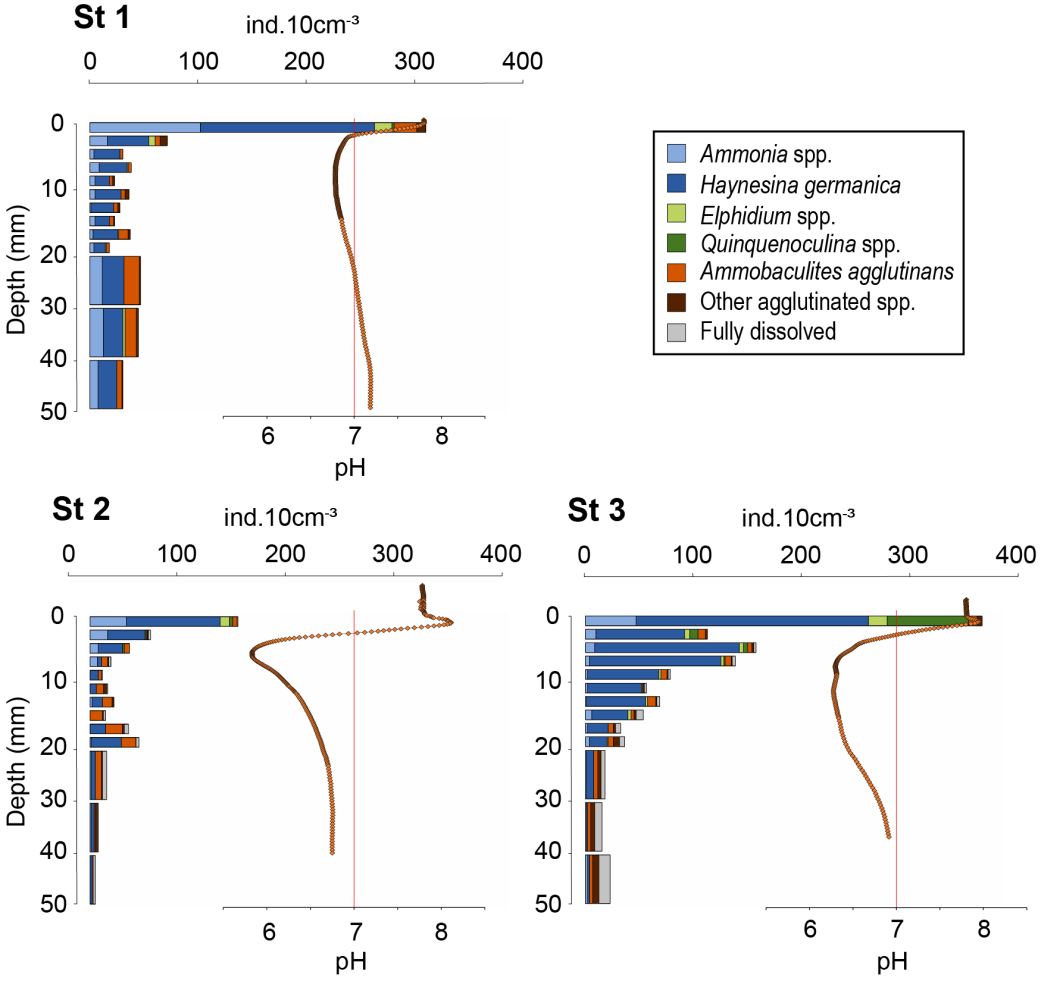

Figure 5. Vertical distributions of living-foraminifera densities per 10 cm³ of sediment at the three stations (>125 µm fraction). *0 is the position of the Sea Water Interface (SWI). Recall of pH microprofiles (orange diamonds) and neutral pH (vertical red line).*

252 **3.2.2 Living Foraminiferal Vertical Distribution**

253 Total densities of CTG-labelled foraminifera in cores 1, 2 and 3 were 1273, 548, and 1431
254 ind.50cm^{-2} respectively. Highest densities were found in the first layer of sediment (0-2 mm
255 depth) for all cores with 295, 137 and 371 ind.10cm^{-3} at stations 1, 2 and 3, respectively (**Figure**
256 **5**), where dioxygen was available and pH was maximal (**Figure 4**).

257 At station 1, total density dropped below 2 mm to stabilize at 30 ± 9 ind.10cm^{-3} (**Figure**
258 **5**). At station 2, the vertical distribution of total densities showed two maxima. The first at the
259 SWI and a second at 18-20 mm depth with 47 ind.10cm^{-3}. A first minimum of 11 ind.10cm^{-3}

https://doi.org/10.5194/bg-2023-169
Preprint. Discussion started: 21 September 2023

was observed at 8-10mm depth close to the lowest pH layer and a second minimum of 5 ind.10cm^{-3} was observed at the bottom of the core. At station 3, after a maximum at the SWI, foraminifera density decreased gradually with depth, following the pH trend, to reach on average 19 ± 4 ind.10cm^{-3} from 20 to 50 mm depth.

At station 1, the ratio of calcareous foraminifera in the living foraminiferal assemblage (C/T) was 0.91 for the SWI (**Table 3**) and around 0.77 ± 0.07 for the layers below. At station 2, C/T was 0.97 of the SWI and on average 0.64 ± 0.16 between 2- and 50-mm depth (**Appendix**). However, agglutinated taxa dominated the assemblages from 10 to 18 mm, just below the pH minimum, with a drop of C/T ratio to 0.39 ± 0.18 (**Appendix**). At station 3, the C/T ratio was 0.97 at the SWI and decreased asymptotically as calcareous foraminiferal densities vanished to reach 0.72 ± 0.15 below 20 mm after the pH minimum zone (**Appendix**).

3.2.3 Calcareous Test Dissolution of Living Foraminifera

Figure 6 shows the dissolution stage (DS) of calcareous foraminifera for three selected layers (0-2 / 6-8 / 40-50 mm) for living assemblages. At station 1, living specimens with calcareous test showed low alteration. The DS remained stable through depth ($p > 0.05$). Specimens with "Intact tests" (DS-0) or "slight surface dissolved tests" (DS-1) represented 90 % of calcareous foraminifera. The strongest dissolution stages were DS-2 ("peeled test") and DS-3 ("cracked test") accounting for less than 10 %.

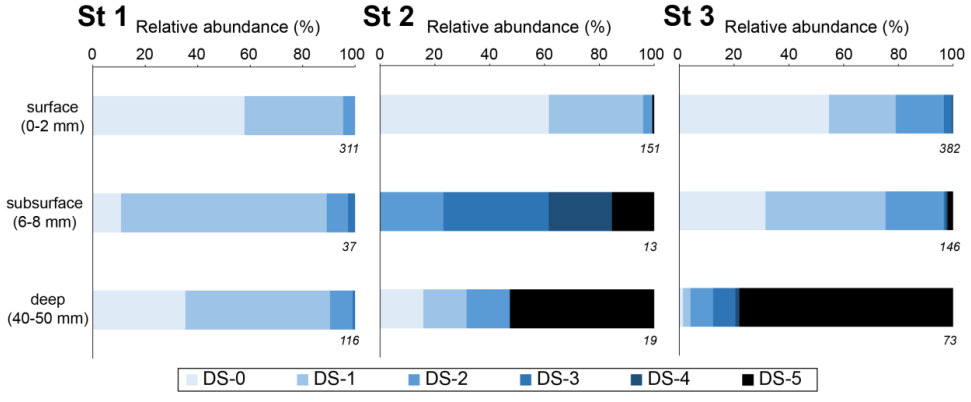

Figure 6. Relative abundance of living benthic foraminifera with calcareous test for each dissolution stage for 10 cm^3 of sediment (Ammonia spp. and H. germanica from the >125 µm fraction). *Three depth levels were analysed: the surface (0-2 mm; oxic zone), the subsurface (6-8 mm; suboxic zone corresponding to pH minimum), and the deeper (40-50 mm; anoxic zone). The numbers on the lower right of the boxes are the total numbers of SEM photographed specimens.*

Conversely, at station 2, many foraminifera were very fragile under manipulation. Numerous "fully dissolved tests" (DS 5) with only the organic lining were observed through depth (50 ind.50cm^{-2}; **Appendix**). At the SWI (0-2 mm layer), DS-0 and DS-1 tests represented 95% of the calcareous test foraminifera in the living assemblage. Only few DS-2 and DS-5 specimens were present. In the subsurface level (6-8-mm depth), corresponding to the most

https://doi.org/10.5194/bg-2023-169
Preprint. Discussion started: 21 September 2023

283 acidic conditions, no DS-0 and DS-1 specimen were observed. DS-4 and DS-5 tests were
284 about 40 % of the calcareous tests observed. At the deepest layer (40-50 mm), DS-5
285 specimens were dominant (>50 %). The surface layer was significantly different ($p < 0.005$)
286 from the two deeper layers that showed no significant differences ($p = 0.267$).

287 At station 3, many foraminifera were fragile under manipulation, and DS-5 specimens
288 were abundant through depth with about 140 ind.50cm^{-2} (**Appendix**). At the SWI (0-2 mm
289 layer) and in the subsurface level (6-8-mm depth), DS-0 and DS-1 specimens represented
290 about 75 % while DS-2 accounted for 20 %. Few specimens of DS-3, DS-4 and DS-5 were
291 observed. At the deepest layer (40-50 mm), DS-5 specimens were the most abundant
292 calcareous tests foraminifera (78 %). The severe DS (DS-3, 4 and 5) were significantly
293 overrepresented in the deep layer than in the surface and subsurface layers ($p < 0.005$). DS
294 were not significantly different between surface and subsurface ($p = 1$).

295 Overall, the exact Fisher's test revealed significant difference dissolution stages among
296 stations ($p<0.005$). The pair-wise Fisher's exact test showed that the low DS (0,1,2) were
297 significantly overrepresented at station 1 compared to the two other stations ($p<0.005$).
298 Furthermore, there were no significant difference between stations 2 and 3 ($p=0.532$).

299 **3.2.4 Calcareous vs. Agglutinated Foraminifera in the Dead Assemblages**
300 Species in the benthic foraminiferal thanatocoenosis were the same as in the living
301 assemblages. At station 1, calcareous taxa dominated agglutinated ones in the dead
302 assemblage with C/T ratio varying from 0.74 to 0.89 (**Table 3**). The proportion of organic lining
303 (DS-5/C) increased slightly with depth, from 0.06 to 0.18. On the other hand, at station 2,
304 agglutinated taxa dominated the dead assemblage in the surface and subsurface levels (C/T
305 ratio of 0.43 and 0.36 respectively) but not in the deepest one even if they remained abundant
306 (0.65; **Table 3**). The DS-5/C ratio was very high in all three depth layers, remaining >0.70. At
307 station 3, C/T ratio remained high in the dead assemblage of both surface and subsurface with
308 0.88, 0.83, and decreased strongly to 0.36 in depth where agglutinated specimens were
309 dominant. The DS-5/C ratio increased with depth, from 0.06 at the surface to 0.95 in the deeper
310 layer.

311 Comparing dead and living assemblages, it can be noted that for station 1, C/T ratio
312 were not very different whatever the depth (**Table 3**). Stations 2 and 3 showed much lower C/T
313 ratios in the dead assemblages indicating a marked loss of calcareous foraminifera during
314 taphonomic processes although this difference is not significant. In addition, stations 2 and 3
315 showed a higher occurrence of DS-5 tests in the dead assemblages resulting in high DS-5/C
316 ratios. In detail, station 2 showed the highest DS-5/C ratio in the subsurface layer (0.96) where
317 pH is minimal, while station 3 showed a strong increase of this ratio in the deepest layer (0.95).

https://doi.org/10.5194/bg-2023-169
Preprint. Discussion started: 21 September 2023

Table 3. Densities of living and dead foraminifera for each depth layer at the three all stations (ind.10 cm^{-3} of sediment). *Depth correspondences: surface (0-2 mm), subsurface (6-8 mm) and deep (4-5 mm). "Calcareous" class includes the DS-5 specimens (fully dissolved test showing the organic lining). A = agglutinated, C = calcareous, ratios are those described in the methods.*

		Living foraminifera					Dead foraminifera				
		Agglutinated (A)	Calcareous (C)	Fully dissolved test (DS-5)	C/T ratio	DS-5/C ratio	Agglutinated (A)	Calcareous (C)	Fully dissolved test (DS-5)	C/T ratio	DS-5/C ratio
St 1	surface [0-2 mm]	30	295	0	0.91	0.00	212	589	38	0.74	0.06
	subsurface [6-8 mm]	3	36	0	0.92	0.00	21	153	22	0.88	0.14
	deep [40-50 mm]	6	26	0	0.81	0.00	94	772	141	0.89	0.18
St 2	surface [0-2 mm]	4	137	1	0.97	0.01	373	282	197	0.43	0.70
	subsurface [6-8 mm]	7	12	2	0.63	0.17	181	104	100	0.36	0.96
	deep [40-50 mm]	1	4	2	0.80	0.50	239	453	327	0.65	0.72
St 3	surface [0-2 mm]	12	371	0	0.97	0.00	58	418	49	0.88	0.12
	subsurface [6-8 mm]	7	137	3	0.95	0.02	45	214	53	0.83	0.25
	deep [40-50 mm]	9	14	11	0.61	0.79	493	274	259	0.36	0.95

4 DISCUSSION

4.1 Cable Bacteria Density and Activity in Mudflats of the Auray Estuary

Oxygen and pH microprofiles recorded at stations 2 and 3 showed the typical fingerprint of CBA: a pH maximum within the oxic zone without oxygen production followed by a significant acidification into the suboxic zone (**Figure 4**; Nielsen et al., 2010; Pfeffer et al., 2012; Risgaard-Petersen et al., 2012; Meysman et al., 2015). The presence of CB at station 2 was further confirmed by the qPCR data. At station 2, the 16S CB copy number was constant within the oxic and suboxic zones (upper first centimetre; **Figure 4**). The calculated filament density of about 70 m.cm^{-3} at this station was in the same order of magnitude than the *in situ* densities reported from the Baltic sea (Marzocchi et al., 2018; Hermans et al., 2019), from bivalve reefs (Malkin et al., 2017), subtidal mudflats (van de Velde et al., 2016) or intertidal salt marshes (Larsen et al., 2015). The geochemical signature at station 1 is less clear regarding Cable Bacteria Activity (CBA). There was no pH peak in the oxic zone and only a moderate acidification within the suboxic zone (ΔpH < 0.1). This acidification was lower than expected if only driven by sulphate reduction and too high to be explained by iron reduction (van Cappellen and Wang, 1996; Soetaert et al., 2007). Therefore, we suggested that it was driven by low CBA. The qPCR data indicated very low CB filament density about 7 m.cm^{-3}. The filament density was in the low range of the *in situ* densities reported from the Baltic sea (Marzocchi et al., 2018; Hermans et al., 2019). The diversity of pH microprofiles observed between the three

https://doi.org/10.5194/bg-2023-169
Preprint. Discussion started: 21 September 2023

342 stations could indicate a contrasted intensity of the CBA between stations. According to the
343 low filament abundance and the low range of pH (ΔpH = 1.0) at station 1, the CBA would be
344 minimal and it would have limited impact on the sediment geochemistry. Conversely, the strong
345 abundance and pH range (ΔpH = 2.4) suggest the most intense CBA at station 2, whereas pH
346 range (ΔpH = 1.8) at station 3 suggests an intermediate to high CBA.

347 Currently, the control factors of spatial and temporal variability of the CB density and
348 the CBA on mudflats are still unresolved. Our observations suggest that *Ulvae* mats observed
349 at stations 2 and 3 during core sampling could play a role on CB development. Several studies
350 showed that macrophyte decay is rather slow compared to mirophytobenthic mineralization
351 and favours free-sulphide production and upward diffusion (Anschutz et al., 2007; Metzger et
352 al., 2007; Cesbron et al., 2014; Delgard et al., 2016). Previous observations confirm the rather
353 high spatial and temporal CBA dynamics already mentioned in the literature (e.g. Seitaj et al.,
354 2015; Lipsewers et al., 2017; Hermans et al., 2019).

355 4.2 Impact of Cable Bacteria on Living Foraminifera

356 The CBA causes pH anomalies that impact sediment geochemistry and lead to the carbonate
357 dissolution process as described in Risgaard-Petersen et al. (2012), Meysmann et al. (2015),
358 van der Velde et al. (2016) and Rao et al. (2016). By analogy, it has been supposed that CBA
359 could also be responsible for foraminifera dissolution (Risgaard-Petersen et al., 2012; Richirt
360 et al., 2022). We showed in **Figure 4** and **Figure 6** that advanced dissolution stages 3, 4 and
361 5 were significantly overrepresented at stations 2 and 3, where acidification was important,
362 compared to station 1 where no DS-5 was observed. More precisely, vertical DS distribution
363 corresponded to vertical acidity variability at stations 2 ($0.01 < DS\text{-}5/C < 0.50$) and 3 ($0.00 <$
364 $DS\text{-}5/C < 0.79$). There is no indication for such depth distribution at station 1 where pH
365 variability was the lowest ($DS\text{-}5/C = 0$). The relative abundance of calcareous specimens over
366 agglutinated (C/T) is very stable along depth at station 1 (0.78 ± 0.07; **Appendix**) whereas this
367 ratio is more variable at stations 2 and 3 (0.65 ± 0.17 and 0.73 ± 0.15 respectively), confirming
368 that pH conditions affect assemblage composition through the under representation of
369 calcareous foraminifera although species diversity is never affected (**Figure 5**). Assuming that
370 acidification intensity in the suboxic zone is due to cable bacteria activity, our data suggest that
371 CB have a drastic effect on the integrity of shells from living benthic foraminifera and potentially
372 on their assemblages. The magnitude of this effect may depend in the CBA intensity and
373 duration throughout the life cycle of foraminifera.

374 Since the dataset of the present study is rather limited, one can examine literature data
375 that provides together oxygen and pH microprofiles with sub-centimetre vertical distribution of
376 living foraminifera in intertidal mudflats first and other benthic environments then. Geochemical

https://doi.org/10.5194/bg-2023-169
Preprint. Discussion started: 21 September 2023

data from an intertidal mudflat of the Arcachon basin in the French Atlantic coast suggest CBA in May 2011 at N station (Cesbron et al., 2016) with a ΔpH = 1.6 and a pH minimum of 6.2 well below the oxic zone at 20-mm depth. At the same station in July 2011, all calcareous benthic foraminifera specimens showed a fully dissolved test with the organic lining remaining (DS-5/C = 1). The assemblage also showed that, *Eggerella scabra*, an agglutinated species, strongly dominated the foraminiferal assemblage at all depths down to 50 mm, except for the 0 to 5 mm layer (C/T = 0.88 ± 0.02 for the uppermost layer; C/T = 0 below). The authors assumed that test dissolution resulted from a strong acidification of the sediments due to an intense remineralisation of the relict roots of *Zostera*. We can assume here that these roots provided the refractory material that enhanced sulphate reduction (Anschutz et al., 2007; Metzger et al., 2007; Cesbron et al., 2014; Delgard et al., 2016), providing enough free-sulphide to favour CB development that drove the dissolution process as it probably happened at stations 2 and 3 of the Auray estuary in the present study. However, Cesbron and co-workers also showed that during winter (February 2011), foraminifera showed less dissolution due to a lower intensity of diagenetic processes including free-sulphide production and probably benthic acidification. These results underline the importance of the temporal variability of diagenetic processes that influence pore water geochemistry including CBA (Seitaj et al., 2015; Lipsewers et al., 2017; Hermans et al., 2019; Malkin et al., 2022), and eventually calcareous test integrity. It also questions about time integration of pH conditions recorded in the foraminifera tests as foraminifera may have mechanisms to buffer pH variations as suggested by different studies (de Nooijer et al., 2009b, 2014; Toyofuku et al., 2017) or vertical migration strategies (Geslin et al., 2004; Pucci et al., 2009; Koho et al., 2011; Hess et al., 2013). It could be assumed that the dissolution of the calcareous foraminifera tests would respond to an integrated dynamics over several months of exposure to the acidity caused by CBA, rather than immediately. These dynamics should be investigated in the future in Auray estuary to better understand differences of dissolution stages observed between stations. It can also be assumed that tolerance to acidification may be species-dependent and needs detailed investigation.

Conversely, a tidal mudflat from another estuarine system of French Atlantic coast seems not to show indices of CBA nor occurrence of dissolution on living foraminifera. Living foraminifera form the Brillantes mudflat of Loire estuary was studied at two stations in September 2012 and April 2013 (Thibault de Chanvalon et al., 2015, 2022). The vertical distribution of living foraminifera reported in the Loire mudflat was similar to the vertical distribution of station 2 reported in the present study with a maximal density at the topmost layer within the oxic zone, a minimal density around 10-mm depth and a second maximum below. However, no foraminiferal test dissolution was reported by Thibault de Chanvalon and co-workers and the foraminiferal assemblages were heavily dominated by calcareous

https://doi.org/10.5194/bg-2023-169
Preprint. Discussion started: 21 September 2023

413 foraminiferal species, resulting in a DS-5/C ratio equal to zero and a C/T ratio about 1.
414 Furthermore, at these stations, pH profiles did not show signs of CBA at different occasions
415 (May 2013, February 2014, June 2018, unpublished data). pH decrease corresponded to
416 oxygen uptake and was below 0.5 units with a minimum about 7.7. No pH peak at the interface
417 was observed in a profile performed in the dark neither. The major difference between these
418 systems is the size of the river that induces significant resuspension-deposition event for the
419 Loire estuary limiting the development of favourable conditions to CB development. In addition,
420 bioturbation seems to be intense at the Brillantes mudflat (Thibault de Chanvalon et al., 2015,
421 2016b, 2017). Another difference between these studies is the absence of macrophytes at the
422 studied stations of the Brillantes mudflat. Finally the size of the catchment area of Loire
423 provides an important flux of suspended particles rich in metallic oxides that will once settled
424 in the mudflat generate a thick layer of sediment where the iron cycle dominates diagenetic
425 processes acting as an efficient “iron curtain” that maintains free-sulphide between 5 to 10 cm
426 depth (Thibault de Chanvalon et al., 2016b, 2016a) to be out of reach for CB. These combined
427 conditions are not favourable to CB development (Malkin et al., 2014, 2017). This, foraminiferal
428 observations strongly suggest the absence of CBA in the studied part of the Brillantes mudflat.
429 This area may be considered as a control station.

430 Other studies reporting calcareous test dissolution of benthic living foraminifera in
431 comparable environments are published but without geochemical data, allowing to discuss
432 potential CBA (Alve and Nagy, 1986; Buzas-Stephens, 2005; Polovodova and Schonfeld,
433 2008; Bentov et al., 2009; de Nooijer et al., 2009; Kurtarkar et al., 2011; Haynert et al., 2012;
434 Schönfeld and Mendes, 2022). Although the hypotheses put forward by these authors on the
435 causes of test dissolution are all plausible (environmental pollution, freshwater inputs, organic
436 matter degradation), they are not strongly explained. Therefore, the absence of pH data
437 (Buzas-Stephens, 2005; Polovodova and Schonfeld, 2008) or its insufficient vertical resolution
438 (Alve and Nagy, 1986; Haynert et al., 2012; Schönfeld and Mendes, 2022) does not exclude
439 the potential involvement of CB in those environments. In the Baltic sea, that could be
440 considered as a sort of giant estuary, Charrieau et al. (2018a), provide pH microprofiles that
441 seem to indicate the absence of CBA. However, these authors observed calcareous test
442 dissolution of living foraminifera and concluded that dissolution may be the consequence of a
443 complex set of environmental factors whose ecological equilibrium can change rapidly in such
444 coastal areas (salinity, oxygen concentration, pH and Ω_{calc}). Laboratory experiments conducted
445 by these authors (Charrieau et al., 2018c), seem to indicate that low salinity may be an
446 important factor on calcareous test dissolution. The difference with estuarine studies discussed
447 above is probably that salinity change dynamics in the Baltic is rather minor compared to

https://doi.org/10.5194/bg-2023-169
Preprint. Discussion started: 21 September 2023

salinity in Auray and Loire that are macrotidal systems with species adapted to such salinity variations.

Considering the increase of observations of cable bacteria activity occurrence in a wide range of marine environments (Malkin et al., 2014; Burdorf et al., 2017) like estuaries, coastal lagoons, salt marshes, marine lakes, tidal and subtidal mudflats, we assume that the impact of CBA on foraminifera community should be strongly considered.

4.3 Impact of Cable Bacteria on Dead Assemblages

Richirt et al. (2022) have assumed that calcareous test dissolution resulting from CBA could be responsible for low densities of calcareous tests in the dead assemblages recorded in sediments of Lake Grevelingen. Our results suggest that acidification caused by CBA strongly affects the calcareous shell integrity and the assemblage composition of living foraminifera before taphonomic processes. Our study also suggests that after foraminifera death, CBA keeps transforming the foraminifera assemblage during test burial confirming the hypothesis formulated by Richirt and coworkers (2022). Comparing C/T and DS-5/C ratios between living and dead assemblages at different depths we relate in detail the impact of pH distribution and therefore CBA to the taphonomic loss. Under a weak CBA (like at station 1), calcareous tests were relatively well preserved. At this station, the community structure between living and dead assemblages varied slightly (C/T ranged from 0.81- to 0.98 in living assemblage and from 0.74- to 0.89 in dead assemblage). The occurrence of dissolution in the living assemblage was nil while in the dead assemblage the DS-5/C ratio increased with depth from 0.06 to 0.18 indicating that the low dissolution generated a relatively slow taphonomic process. Calcareous tests dominated both living and dead assemblages with an increase of this trend with depth in the dead assemblage confirming the good preservation of calcareous foraminifera. Where CBA was moderate (like at station 3), the dissolution effect on the thanatocoenosis was gradual with depth. Calcareous test density decreased through the wide acidic layer (C/T decrease from above 0.8 to 0.36 at 50-mm depth) and there was an accumulation of fully dissolved tests showing only their organic linings in dead foraminiferal assemblages at depth (DS-5/C of 0.95). This feature suggests that the moderate dissolution generated a gradual taphonomic process leading to a noticeable calcareous loss with depth. Eventually, under a strong and intense CBA (like at station 2), the dissolution effect occurred mostly within the restricted acidic layer. The calcareous tests disappeared from the dead foraminiferal assemblage in this subsurface layer while the fully dissolved tests showing only their organic linings and agglutinated tests accumulated (C/T = 0.37 and DS-5/C = 0.96). At depth, the dead foraminiferal assemblage showed fairly high densities that are comparable to stations where CBA was less intense. As the living specimens were quite rare, such accumulation of dead tests suggested that somehow they bypassed the acidic firewall of the suboxic layer. If tests arrived at depth through

https://doi.org/10.5194/bg-2023-169
Preprint. Discussion started: 21 September 2023

sedimentary burial the acidic firewall was possibly not active in a recent past. If CBA is not recent, physical or biological reworking buried sufficiently fast to preserve tests from corrosive conditions and mechanic crumbling. At this stage, these hypotheses cannot be assessed. One can note the high concentration of dead fully dissolved tests in the first 2 mm (0.70) where pH is the most alkaline suggesting that sedimentary reworking may have brought dead specimens from the subsurface acidic layer to the surface. Further studies on dead assemblages are needed to statistically validate the CBA vs. calcareous test loss relationship.

With low pH in pore water, the dissolution process resulting from CBA suggests an imprint on taphonomy and on historical records yet to be explored. Dissolution of living and dead calcareous test foraminifera due to CBA may be taken into account in interpretations of foraminiferal assemblages in historical studies. As proposed in Richirt et al. (2022), historical records of benthic foraminifera could also be used to reconstruct past CBA and determine the age of the first CB occurrence in the studied environments. Therefore, associating it with major environmental changes, light could be shed on the original factors of this bacterial spreading discovered only ten years ago.

5 Conclusion

This original study strongly suggests that sediment acidification caused by CBA could be responsible for significant calcareous test foraminifera dissolution patterns. As a result, proportions of calcareous test would change in both living and dead assemblages. The proportion of fully dissolved tests showing only their organic linings would increase in the living assemblages in the suboxic and anoxic zones of the sediment, as well as in the thanatocoenosis. The spatial dynamics of calcareous test dissolution in mudflats described in the present study seems to be the consequence of CBA which leads to a wide range of pore water pH in the suboxic zone of sediment.

Now that we have an idea of the potential impact of this bacterial activity on foraminiferal assemblages and on calcareous test preservation, we are entitled to ask what implications this might have for environmental interpretations of data from their use as paleoproxies, or bioindicators. In order to better understand this impact, it would be relevant to explore *in situ* and *in vitro* the effect of CBA at several time scales on the resilience of foraminiferal communities to learn more about the integration of their response in the historic/fossil record. Eventually, we should be able to provide a historical retrospective on the presence of CB in marine sediments and their impact on the benthic meiofauna. In this perspective, we should combine such studies with the development of biomarkers of these chemolithoautotrophic bacteria or of ancient eDNA.

https://doi.org/10.5194/bg-2023-169
Preprint. Discussion started: 21 September 2023

Data availability. All of the data are published within this paper and in the Supplement. The raw data used to make the figures are available on request.

Author contributions. Maxime DAVIRAY (foraminiferal and geochemical analysis, writing, review and editing), Emmanuelle GESLIN (head of CB-For CNRS project, foraminiferal analysis, writing, review and editing), Nils RISGAARD-PETERSEN (statistical inference, writing, review and editing), Vincent SCHOLZ (qPCR proceeding, review and editing), Marie FOUET (field work, review and editing), Edouard METZGER (microprofile acquisition, writing, review and editing).

Competing interests. At least one of the (co-)authors is a member of the editorial board of Biogeosciences.

Acknowledgments. The authors are grateful to Sophie QUINCHARD for assistance with the foraminifera picking, Sophie SANCHEZ for sample splitting (LPG, Université d'Angers) and Romain MALLET (SCIAM, Université d'Angers) for the achievement of a part of the SEM imaging. Susanne NIELSEN and Ian MARSHALL (Aarhus University) are thanked for assistance with the qPCR analysis. The authors are grateful to Frans JORISSEN for field work, and his advice for the writing process (LPG, Université d'Angers). The authors thank the participants to the field trips (2019 and 2020).

Financial support. The authors received funding from the CNRS-INSU (program LEFE-CYBER, project CB-FOR), from the Angers University and from the OFB (project FORESTAT).

REFERENCES

Alve, E., and Nagy, J. (1986). Estuarine foraminiferal distribution in Sandebukta, a branch of the Oslo Fjord (Norway). *Journal of Foraminiferal Research - J FORAMIN RES* 16, 261–284. doi: 10.2113/gsjfr.16.4.261.

Anschutz, P., Chaillou, G., and Lecroart, P. (2007). Phosphorus diagenesis in sediment of the Thau Lagoon. *Estuarine, Coastal and Shelf Science* 72, 447–456. doi: 10.1016/j.ecss.2006.11.012.

Balsamo, M., Semprucci, F., Frontalini, F., and Coccioni, R. (2012). "Meiofauna as a Tool for Marine Ecosystem Biomonitoring," in *Marine ecosystems* (InTech), 77–104.

Bentov, S., Brownlee, C., and Erez, J. (2009). The role of seawater endocytosis in the biomineralization process in calcareous foraminifera. *Proceedings of the National Academy of Sciences* 106, 21500–21504. doi: 10.1073/pnas.0906636106.

Bernhard, J. M., and Bowser, S. S. (1996). Novel epifluorescence microscopy method to determine life position of foraminifera in sediments. *J. Micropalaeontol.* 15, 68–68. doi: 10.1144/jm.15.1.68.

Bernhard, J. M., Ostermann, D. R., Williams, D. S., and Blanks, J. K. (2006). Comparison of two methods to identify live benthic foraminifera: A test between Rose Bengal and CellTracker Green with implications for stable isotope paleoreconstructions: Foraminifera Viability Method Comparison. *Paleoceanography* 21. doi: 10.1029/2006PA001290.

Boudagher-Fadel, M. K. (2018). "Biology and Evolutionary History of Larger Benthic Foraminifera," in *Evolution and Geological Significance of Larger Benthic Foraminifera* (UCL Press), 1–44. doi: 10.2307/j.ctvqhsq3.3.

https://doi.org/10.5194/bg-2023-169
Preprint. Discussion started: 21 September 2023

560 Burdorf, L. D. W., Tramper, A., Seitaj, D., Meire, L., Hidalgo-Martinez, S., Zetsche, E.-M., et
561 al. (2017). Long-distance electron transport occurs globally in marine sediments.
562 *Biogeosciences* 14, 683–701. doi: 10.5194/bg-14-683-2017.

563 Buzas-Stephens, P. (2005). Population Dynamics and Dissolution of Foraminifera in Nueces
564 Bay, Texas. *The Journal of Foraminiferal Research* 35, 248–258. doi:
565 10.2113/35.3.248.

566 Cesbron, F., Metzger, E., Launeau, P., Deflandre, B., Delgard, M.-L., Thibault de Chanvalon,
567 A., et al. (2014). Simultaneous 2D Imaging of Dissolved Iron and Reactive Phosphorus
568 in Sediment Porewaters by Thin-Film and Hyperspectral Methods. *Environ. Sci.*
569 *Technol.* 48, 2816–2826. doi: 10.1021/es404724r.

570 Cesbron, F., Geslin, E., Jorissen, F. J., Delgard, M. L., Charrieau, L., Deflandre, B., et al.
571 (2016). Vertical distribution and respiration rates of benthic foraminifera: Contribution
572 to aerobic remineralization in intertidal mudflats covered by *Zostera noltei* meadows.
573 *Estuarine, Coastal and Shelf Science* 179, 23–38. doi: 10.1016/j.ecss.2015.12.005.

574 Charrieau, L. M., Bryngemark, L., Hansson, I., and Filipsson, H. L. (2018a). Improved wet
575 splitter for micropalaeontological analysis, and assessment of uncertainty using data
576 from splitters. *J. Micropalaeontol.* 37, 191–194. doi: 10.5194/jm-37-191-2018.

577 Charrieau, L. M., Filipsson, H. L., Ljung, K., Chierici, M., Knudsen, K. L., and Kritzberg, E.
578 (2018b). The effects of multiple stressors on the distribution of coastal benthic
579 foraminifera: A case study from the Skagerrak-Baltic Sea region. *Marine*
580 *Micropaleontology* 139, 42–56. doi: 10.1016/j.marmicro.2017.11.004.

581 Charrieau, L. M., Filipsson, H. L., Nagai, Y., Kawada, S., Ljung, K., Kritzberg, E., et al. (2018c).
582 Decalcification and survival of benthic foraminifera under the combined impacts of
583 varying pH and salinity. *Marine Environmental Research* 138, 36–45. doi:
584 10.1016/j.marenvres.2018.03.015.

585 Choquel, C., Geslin, E., Metzger, E., Filipsson, H. L., Risgaard-Petersen, N., Launeau, P., et
586 al. (2021). Denitrification by benthic foraminifera and their contribution to N-loss from a
587 fjord environment. *Biogeosciences* 18, 327–341. doi: 10.5194/bg-18-327-2021.

588 Corliss, B. H., and Honjo, S. (1981). Dissolution of Deep-Sea Benthonic Foraminifera.
589 *Micropaleontology* 27, 356. doi: 10.2307/1485191.

590 de Nooijer, L. J., Toyofuku, T., and Kitazato, H. (2009). Foraminifera promote calcification by
591 elevating their intracellular pH. *Proceedings of the National Academy of Sciences* 106,
592 15374–15378. doi: 10.1073/pnas.0904306106.

593 de Nooijer, L. J., Spero, H. J., Erez, J., Bijma, J., and Reichart, G. J. (2014). Biomineralization
594 in perforate foraminifera. *Earth-Science Reviews* 135, 48–58. doi:
595 10.1016/j.earscirev.2014.03.013.

596 Debenay, J.-P., Guillou, J.-J., Redois, F., and Geslin, E. (2000). “Distribution Trends of
597 Foraminiferal Assemblages in Paralic Environments,” in *Environmental*
598 *Micropaleontology: The Application of Microfossils to Environmental Geology* Topics in
599 Geobiology., ed. R. E. Martin (Boston, MA: Springer US), 39–67. doi: 10.1007/978-1-
600 4615-4167-7_3.

601 Debenay, J.-P., Bicchi, E., Goubert, E., and Armynot du Châtelet, E. (2006). Spatio-temporal
602 distribution of benthic foraminifera in relation to estuarine dynamics (Vie estuary,

https://doi.org/10.5194/bg-2023-169
Preprint. Discussion started: 21 September 2023

603 Vendée, W France). *Estuarine, Coastal and Shelf Science* 67, 181–197. doi:
604 10.1016/j.ecss.2005.11.014.

605 Delgard, M. L., Deflandre, B., Kochoni, E., Avaro, J., Cesbron, F., Bichon, S., et al. (2016).
606 Biogeochemistry of dissolved inorganic carbon and nutrients in seagrass (Zostera
607 noltei) sediments at high and low biomass. *Estuarine, Coastal and Shelf Science* 179,
608 12–22. doi: 10.1016/j.ecss.2016.01.012.

609 Durand, M., Mojtahid, M., Maillet, G. M., Baltzer, A., Schmidt, S., Blet, S., et al. (2018). Late
610 Holocene record from a Loire River incised paleovalley (French inner continental shelf):
611 Insights into regional and global forcing factors. *Palaeogeography, Palaeoclimatology,*
612 *Palaeoecology* 511, 12–28. doi: 10.1016/j.palaeo.2018.06.035.

613 Envlit Bassin Loire-Bretagne. Available online: https://wwz.ifremer.fr/envlit/DCE/La-DCE-par-
614 bassin/Bassin-Loire-Bretagne (accessed on 05 May 2021).

615 Fouet, M. P. A., Singer, D., Coynel, A., Héliot, S., Howa, H., Lalande, J., et al. (2022).
616 Foraminiferal Distribution in Two Estuarine Intertidal Mudflats of the French Atlantic
617 Coast: Testing the Marine Influence Index. *Water* 14, 645. doi: 10.3390/w14040645.

618 Geelhoed, J. S., van de Velde, S. J., and Meysman, F. J. R. (2020). Quantification of Cable
619 Bacteria in Marine Sediments via qPCR. *Frontiers in Microbiology* 11, 1506. doi:
620 10.3389/fmicb.2020.01506.

621 Geslin, E., Heinz, P., Jorissen, F., and Hemleben, Ch. (2004). Migratory responses of deep-
622 sea benthic foraminifera to variable oxygen conditions: laboratory investigations.
623 *Marine Micropaleontology* 53, 227–243. doi: 10.1016/j.marmicro.2004.05.010.

624 Gonzales, M. V., De Almeida, F. K., Costa, K. B., Santarosa, A. C. A., Camillo, E., De Quadros,
625 J. P., et al. (2017). Helpd Index: *Hoeglundina elegans* Preservation Index for Marine
626 Sediments in the Western South Atlantic. *Journal of Foraminiferal Research* 47, 56–
627 69. doi: 10.2113/gsjfr.47.1.56.

628 Hansen, H. J. (1999). “Shell construction in modern calcareous Foraminifera,” in *Modern*
629 *Foraminifera* (Dordrecht: Springer Netherlands), 57–70. doi: 10.1007/0-306-48104-
630 9_4.

631 Haynert, K., Schönfeld, J., Riebesell, U., and Polovodova, I. (2011). Biometry and dissolution
632 features of the benthic foraminifer Ammonia aomoriensis at high pCO_2. *Marine Ecology*
633 *Progress Series* 432, 53–67. doi: 10.3354/meps09138.

634 Haynert, K., Schönfeld, J., Polovodova-Asteman, I., and Thomsen, J. (2012). The benthic
635 foraminiferal community in a naturally CO_2-rich coastal habitat of the southwestern
636 Baltic Sea. *Biogeosciences* 9, 4421–4440. doi: 10.5194/bg-9-4421-2012.

637 Haynert, K., Schönfeld, J., Schiebel, R., Wilson, B., and Thomsen, J. (2014). Response of
638 benthic foraminifera to ocean acidification in their natural sediment environment: a
639 long-term culturing experiment. *Biogeosciences* 11, 1581–1597. doi: 10.5194/bg-11-
640 1581-2014.

641 Haynes, J. R. (1981). *Foraminifera*. Springer.

642 Hermans, M., Lenstra, W. K., Hidalgo-Martinez, S., van Helmond, N. A. G. M., Witbaard, R.,
643 Meysman, F. J. R., et al. (2019). Abundance and Biogeochemical Impact of Cable
644 Bacteria in Baltic Sea Sediments. *Environ. Sci. Technol.* 53, 7494–7503. doi:
645 10.1021/acs.est.9b01665.

https://doi.org/10.5194/bg-2023-169
Preprint. Discussion started: 21 September 2023

646 Hess, S., Alve, E., Trannum, H. C., and Norling, K. (2013). Benthic foraminiferal responses to
647 water-based drill cuttings and natural sediment burial: Results from a mesocosm
648 experiment. *Marine Micropaleontology* 101, 1–9. doi: 10.1016/j.marmicro.2013.03.004.

649 Jorissen, F. J., Fouet, M. P. A., Singer, D., and Howa, H. (2022). The Marine Influence Index
650 (MII): A Tool to Assess Estuarine Intertidal Mudflat Environments for the Purpose of
651 Foraminiferal Biomonitoring. *Water* 14, 676. doi: 10.3390/w14040676.

652 Jorissen, F. J., Fouet, M. P. A., Armynot du Châtelet, E., Barras, C., Bouchet, V. M. P., Daviray,
653 M., et al. (2023). *Foraminifères estuariens de la façade atlantique française - Guide de*
654 *détermination*. Université d'Angers; OFB.

655 Kassambara A (2022). _rstatix: Pipe-Friendly Framework for Basic Statistical Tests_. R
656 package version 0.7.1, https://CRAN.R-project.org/package=rstatix.

657 Katz, M. E., Cramer, B. S., Franzese, A., Hönisch, B., Miller, K. G., Rosenthal, Y., et al. (2010).
658 Traditional and Emerging Geochemical Proxies in Foraminifera. *Journal of*
659 *Foraminiferal Research* 40, 165–192. doi: 10.2113/gsjfr.40.2.165.

660 Keul, N., Langer, G., Thoms, S., de Nooijer, L. J., Reichart, G.-J., and Bijma, J. (2017).
661 Exploring foraminiferal Sr/Ca as a new carbonate system proxy. *Geochimica et*
662 *Cosmochimica Acta* 202, 374–386. doi: 10.1016/j.gca.2016.11.022.

663 Koho, K. A., Piña-Ochoa, E., Geslin, E., and Risgaard-Petersen, N. (2011). Vertical migration,
664 nitrate uptake and denitrification: survival mechanisms of foraminifers (Globobulimina
665 turgida) under low oxygen conditions: Survival mechanisms of foraminifers. *FEMS*
666 *Microbiology Ecology* 75, 273–283. doi: 10.1111/j.1574-6941.2010.01010.x.

667 Kurtarkar, S. R., Nigam, R., Saraswat, R., and Linshy, V. N. (2011). Regenaration and
668 Abnormality in Benthic Foraminiefra *Rosalina leei*: Implications in Reconstructing Past
669 Salinity Changes. *Rivista Italiana Di Paleontologia e Stratigrafia*, 189-196.

670 Langlet, D., Geslin, E., Baal, C., Metzger, E., Lejzerowicz, F., Riedel, B., et al. (2013).
671 Foraminiferal survival after long-term *in situ* experimentally induced anoxia.
672 *Biogeosciences* 10, 7463–7480. doi: 10.5194/bg-10-7463-2013.

673 Langlet, D., Baal, C., Geslin, E., Metzger, E., Zuschin, M., Riedel, B., et al. (2014).
674 Foraminiferal species responses to in situ, experimentally induced anoxia in the
675 Adriatic Sea. *Biogeosciences* 11, 1775–1797. doi: 10.5194/bg-11-1775-2014.

676 Le Cadre, V. (2003). Low pH Effects on *Ammonia becarii* Test Deformation: Implications for
677 Using Test deformations as a Pollution Indicator. *The Journal of Foraminiferal*
678 *Research* 33, 1–9. doi: 10.2113/0330001.

679 Lipsewers, Y. A., Vasquez-Cardenas, D., Seitaj, D., Schauer, R., Hidalgo-Martinez, S.,
680 Sinninghe Damsté, J. S., et al. (2017). Impact of Seasonal Hypoxia on Activity and
681 Community Structure of Chemolithoautotrophic Bacteria in a Coastal Sediment. *Appl*
682 *Environ Microbiol* 83. doi: 10.1128/AEM.03517-16.

683 Malkin, S. Y., Rao, A. M., Seitaj, D., Vasquez-Cardenas, D., Zetsche, E.-M., Hidalgo-Martinez,
684 S., et al. (2014). Natural occurrence of microbial sulphur oxidation by long-range
685 electron transport in the seafloor. *ISME J* 8, 1843–1854. doi: 10.1038/ismej.2014.41.

https://doi.org/10.5194/bg-2023-169
Preprint. Discussion started: 21 September 2023

686 Malkin, S. Y., Seitaj, D., Burdorf, L. D. W., Nieuwhof, S., Hidalgo-Martinez, S., Tramper, A., et
687 al. (2017). Electrogenic Sulfur Oxidation by Cable Bacteria in Bivalve Reef Sediments.
688 *Front. Mar. Sci.* 4. doi: 10.3389/fmars.2017.00028.

689 Malkin, S. Y., Liau, P., Kim, C., Hantsoo, K. G., Gomes, M. L., and Song, B. (2022). Contrasting
690 controls on seasonal and spatial distribution of marine cable bacteria (Candidatus
691 Electrothrix) and Beggiatoaceae in seasonally hypoxic Chesapeake Bay. *Limnology*
692 *and Oceanography* 67, 1357–1373. doi: 10.1002/lno.12087.

693 Martin, R. E. (2000). *Environmental Micropaleontology: The Application of Microfossils to*
694 *Environmental Geology*. Kluwer Academic/Plenum Publishers. Springer Available at:
695 https://doi.org/10.1007/978-1-4615-4167-7.

696 Marzocchi, U., Trojan, D., Larsen, S., Louise Meyer, R., Peter Revsbech, N., Schramm, A., et
697 al. (2014). Electric coupling between distant nitrate reduction and sulfide oxidation in
698 marine sediment. *ISME J* 8, 1682–1690. doi: 10.1038/ismej.2014.19.

699 Metzger, E., Simonucci, C., Viollier, E., Sarazin, G., Prévot, F., and Jézéquel, D. (2007).
700 Benthic response to shellfish farming in Thau lagoon: Pore water signature. *Estuarine,*
701 *Coastal and Shelf Science* 72, 406–419. doi: 10.1016/j.ecss.2006.11.011.

702 Meysman, F. J. R., Risgaard-Petersen, N., Malkin, S. Y., and Nielsen, L. P. (2015). The
703 geochemical fingerprint of microbial long-distance electron transport in the seafloor.
704 *Geochimica et Cosmochimica Acta* 152, 122–142. doi: 10.1016/j.gca.2014.12.014.

705 Mojtahid, M., Jorissen, F., Durrieu, J., Galgani, F., Howa, H., Redois, F., et al. (2006). Benthic
706 foraminifera as bio-indicators of drill cutting disposal in tropical east Atlantic outer shelf
707 environments. *Marine Micropaleontology* 61, 58–75. doi:
708 10.1016/j.marmicro.2006.05.004.

709 Murray, J. W. (2006). *Ecology and Applications of Benthic Foraminifera*. Cambridge University
710 Press.

711 Nielsen, L. P., Risgaard-Petersen, N., Fossing, H., Christensen, P. B., and Sayama, M. (2010).
712 Electric currents couple spatially separated biogeochemical processes in marine
713 sediment. *Nature* 463, 1071–1074. doi: 10.1038/nature08790.

714 O'Brien, P. A. J., Polovodova Asteman, I., and Bouchet, V. M. P. (2021). Benthic Foraminiferal
715 Indices and Environmental Quality Assessment of Transitional Waters: A Review of
716 Current Challenges and Future Research Perspectives. *Water* 13, 1898. doi:
717 10.3390/w13141898.

718 Office Français De La Biodiversité Découvrir Les Estuaires de La Façade Manche/Atlantique
719 | Le Portail Technique De l'OFB. Available online:
720 https://professionnels.ofb.fr/fr/node/276 (accessed on 05 May 2022).

721 Patterson, R. T., and Fishbein, E. (1989). Re-examination of the statistical methods used to
722 determine the number of point counts needed for micropaleontological quantitative
723 research. *J. Paleontol.* 63, 245–248. doi: 10.1017/S0022336000019272.

724 Pfeffer, C., Larsen, S., Song, J., Dong, M., Besenbacher, F., Meyer, R. L., et al. (2012).
725 Filamentous bacteria transport electrons over centimetre distances. *Nature* 491, 218–
726 221. doi: 10.1038/nature11586.

https://doi.org/10.5194/bg-2023-169
Preprint. Discussion started: 21 September 2023

Polovodova, I., and Schonfeld, J. (2008). Foraminiferal Test Abnormalities in the Western Baltic Sea. *The Journal of Foraminiferal Research* 38, 318–336. doi: 10.2113/gsjfr.38.4.318.

Pucci, F., Geslin, E., Barras, C., Morigi, C., Sabbatini, A., Negri, A., et al. (2009). Survival of benthic foraminifera under hypoxic conditions: Results of an experimental study using the CellTracker Green method. *Marine Pollution Bulletin* 59, 336–351. doi: 10.1016/j.marpolbul.2009.08.015.

R Core Team (2022). R: A language and environment for statistical computing. R Foundation for Statistical Computing, Vienna, Austria. URL https://www.R-project.org/

Rao, A. M. F., Malkin, S. Y., Hidalgo-Martinez, S., and Meysman, F. J. R. (2016). The impact of electrogenic sulfide oxidation on elemental cycling and solute fluxes in coastal sediment. *Geochimica et Cosmochimica Acta* 172, 265–286. doi: 10.1016/j.gca.2015.09.014.

Revsbech, N. P., and Jørgensen, B. B. (1986). “Microelectrodes: Their Use in Microbial Ecology,” in *Advances in Microbial Ecology* Advances in Microbial Ecology., ed. K. C. Marshall (Boston, MA: Springer US), 293–352. doi: 10.1007/978-1-4757-0611-6_7.

Revsbech, N. P. (1989). An oxygen microsensor with a guard cathode. *Limnol. Oceanogr.* 34, 474–478. doi: 10.4319/lo.1989.34.2.0474.

Richirt, J., Guihéneuf, A., Mouret, A., Schweizer, M., Slomp, C. P., and Jorissen, F. J. (2022). A historical record of benthic foraminifera in seasonally anoxic Lake Grevelingen, the Netherlands. *Palaeogeography, Palaeoclimatology, Palaeoecology* 599, 111057. doi: 10.1016/j.palaeo.2022.111057.

Risgaard-Petersen, N., Revil, A., Meister, P., and Nielsen, L. P. (2012). Sulfur, iron-, and calcium cycling associated with natural electric currents running through marine sediment. *Geochimica et Cosmochimica Acta* 92, 1–13. doi: 10.1016/j.gca.2012.05.036.

Risgaard-Petersen, N., Damgaard, L. R., Revil, A., and Nielsen, L. P. (2014). Mapping electron sources and sinks in a marine biogeobattery. *Journal of Geophysical Research: Biogeosciences* 119, 1475–1486. doi: 10.1002/2014JG002673.

Risgaard-Petersen, N., Kristiansen, M., Frederiksen, R. B., Dittmer, A. L., Bjerg, J. T., Trojan, D., et al. (2015). Cable Bacteria in Freshwater Sediments. *Appl Environ Microbiol* 81, 6003–6011. doi: 10.1128/AEM.01064-15.

Schönfeld, J., and Mendes, I. (2022). Benthic foraminifera and pore water carbonate chemistry on a tidal flat and salt marsh at Ria Formosa, Algarve, Portugal. *Estuarine, Coastal and Shelf Science* 276, 108003. doi: 10.1016/j.ecss.2022.108003.

Seitaj, D., Schauer, R., Sulu-Gambari, F., Hidalgo-Martinez, S., Malkin, S. Y., Burdorf, L. D. W., et al. (2015). Cable bacteria generate a firewall against euxinia in seasonally hypoxic basins. *Proc Natl Acad Sci USA* 112, 13278–13283. doi: 10.1073/pnas.1510152112.

Soetaert, K., Hofmann, A. F., Middelburg, J. J., Meysman, F. J. R., and Greenwood, J. (2007). The effect of biogeochemical processes on pH. *Marine Chemistry* 105, 30–51. doi: 10.1016/j.marchem.2006.12.012.

https://doi.org/10.5194/bg-2023-169
Preprint. Discussion started: 21 September 2023

769 Thibault de Chanvalon, A., Metzger, E., Mouret, A., Cesbron, F., Knoery, J., Rozuel, E., et al.
770 (2015). Two-dimensional distribution of living benthic foraminifera in anoxic sediment
771 layers of an estuarine mudflat (Loire Estuary, France). Biogeochemistry: Sediment doi:
772 10.5194/bgd-12-10311-2015.

773 Thibault de Chanvalon, A., Metzger, E., Mouret, A., Knoery, J., Chiffoleau, J.-F., and Brach-
774 Papa, C. (2016a). Particles transformation in estuaries: Fe, Mn and REE signatures
775 through the Loire Estuary. *Journal of Sea Research* 118, 103–112. doi:
776 10.1016/j.seares.2016.11.004.

777 Thibault de Chanvalon, A., Mouret, A., Knoery, J., Geslin, E., Péron, O., and Metzger, E.
778 (2016b). Manganese, iron and phosphorus cycling in an estuarine mudflat, Loire,
779 France. *Journal of Sea Research* 118, 92–102. doi: 10.1016/j.seares.2016.10.004.

780 Thibault de Chanvalon, A., Metzger, E., Mouret, A., Knoery, J., Geslin, E., and Meysman, F.
781 J. R. (2017). Two dimensional mapping of iron release in marine sediments at
782 submillimetre scale. *Marine Chemistry* 191, 34–49. doi:
783 10.1016/j.marchem.2016.04.003.

784 Thibault de Chanvalon, A., Geslin, E., Mojtahid, M., Métais, I., Méléder, V., and Metzger, E.
785 (2022). Multiscale analysis of living benthic foraminiferal heterogeneity: Ecological
786 advances from an intertidal mudflat (Loire estuary, France). *Continental Shelf*
787 *Research* 232, 104627. doi: 10.1016/j.csr.2021.104627.

788 Toyofuku, T., Matsuo, M. Y., de Nooijer, L. J., Nagai, Y., Kawada, S., Fujita, K., et al. (2017).
789 Proton pumping accompanies calcification in foraminifera. *Nat Commun* 8, 14145. doi:
790 10.1038/ncomms14145.

791 van Cappellen, P., and Wang, Y. (1996). Cycling of iron and manganese in surface sediments:
792 A general theory for the coupled transport and reaction of carbon, oxygen, nitrogen,
793 sulfur, iron, and manganese. *American Journal of Science* 296, 197–243.

794 van de Velde, S., Lesven, L., Burdorf, L. D. W., Hidalgo-Martinez, S., Geelhoed, J. S., Van
795 Rijswijk, P., et al. (2016). The impact of electrogenic sulfur oxidation on the
796 biogeochemistry of coastal sediments: A field study. *Geochimica et Cosmochimica*
797 *Acta* 194, 211–232. doi: 10.1016/j.gca.2016.08.038.

798 World Register of Marine Species. Available online:
799 https://www.marinespecies.org/index.php (assessed on 05 May 2022).

800 ***Appendix.*** *Foraminiferal absolute densities and ratios in the Auray estuary for the three stations.*

	Depth layer	Layer volume (cm-3)	*Haynesina germanica*	*Ammonia* spp.	Elphidium spp.	*Quinqueloculina* spp.	*DS-5 specimen*	*Ammobaculites agglutinans*	Other agglutinans	Total	C/T ratio	DS-5/C ratio
St 1	[0-2 mm]	10.6	179	113	18	2	0	23	9	344	0.91	0.00
	[2-4 mm]	10.6	42	18	6	0	0	5	7	78	0.85	0.00

https://doi.org/10.5194/bg-2023-169
Preprint. Discussion started: 21 September 2023

	[4-6 mm]	10.6	26	4	0	0	0	3	0	33	0.91	0.00
	[6-8 mm]	10.6	28	9	1	0	0	3	0	41	0.93	0.00
	[8-10 mm]	10.6	15	5	0	0	0	3	2	25	0.80	0.00
	[10-12 mm]	10.6	26	5	0	0	0	4	4	39	0.79	0.00
	[12-14 mm]	10.6	23	1	0	0	0	4	2	30	0.80	0.00
	[14-16 mm]	10.6	15	5	0	0	0	4	1	25	0.80	0.00
	[16-18 mm]	10.6	25	3	1	0	0	9	2	40	0.73	0.00
	[18-20 mm]	10.6	12	4	1	0	0	3	0	20	0.85	0.00
	[20-30 mm]	52.8	110	61	2	0	0	77	6	256	0.68	0.00
	[30-40 mm]	52.8	99	67	11	0	2	57	9	245	0.73	0.01
	[40-50 mm]	52.8	93	42	2	0	0	28	4	169	0.81	0.00
St 2	[0-2 mm]	10.6	95	37	9	3	1	4	0	149	0.97	0.01
	[2-4 mm]	10.6	38	18	1	0	2	1	1	61	0.97	0.03
	[4-6 mm]	10.6	24	8	2	0	0	5	0	39	0.87	0.00
	[6-8 mm]	10.6	4	7	0	0	2	6	1	20	0.65	0.15
	[8-10 mm]	10.6	8	0	0	0	1	3	0	12	0.75	0.11
	[10-12 mm]	10.6	6	0	0	0	1	7	3	17	0.41	0.14
	[12-14 mm]	10.6	11	2	0	0	0	10	2	25	0.52	0.00
	[14-16 mm]	10.6	0	0	0	0	2	13	1	16	0.13	1.00
	[16-18 mm]	10.6	16	0	0	0	4	17	2	39	0.51	0.20
	[18-20 mm]	10.6	31	1	0	0	3	15	0	50	0.70	0.09
	[20-30 mm]	52.8	22	6	2	0	20	33	6	89	0.56	0.40
	[30-40 mm]	52.8	15	5	0	0	4	5	8	37	0.65	0.17
	[40-50 mm]	52.8	9	0	0	0	10	5	1	25	0.76	0.53

https://doi.org/10.5194/bg-2023-169
Preprint. Discussion started: 21 September 2023

St 3	[0-2 mm]	10.6	238	52	19	83	0	8	5	405	0.97	0.00
	[2-4 mm]	10.6	91	11	5	8	0	7	2	124	0.93	0.00
	[4-6 mm]	10.6	148	9	4	4	2	4	2	173	0.97	0.01
	[6-8 mm]	10.6	133	4	3	1	3	6	1	151	0.95	0.02
	[8-10 mm]	10.6	73	2	2	0	2	6	1	86	0.92	0.03
	[10-12 mm]	10.6	55	2	1	0	2	1	1	62	0.97	0.03
	[12-14 mm]	10.6	60	1	2	0	3	8	1	75	0.88	0.05
	[14-16 mm]	10.6	37	6	3	0	7	3	2	58	0.91	0.13
	[16-18 mm]	10.6	21	2	0	0	5	5	2	35	0.80	0.18
	[18-20 mm]	10.6	18	4	1	0	5	5	6	39	0.72	0.18
	[20-30 mm]	52.8	38	4	0	0	21	20	16	99	0.64	0.33
	[30-40 mm]	52.8	7	4	1	0	35	15	19	81	0.58	0.74
	[40-50 mm]	52.8	8	9	1	0	57	15	32	122	0.61	0.76

801